

Effect of substitution of basalt for quartz in triaxial porcelain

Fatma A. Firat, Ediz Ercek and Senol Yilmaz*

Sakarya University Engineering Faculty, Department of Metallurgy and Materials Engineering, Esentepe Campus, 54187 Sakarya, Turkey

Porcelain is a material produced from kaolinitic clay, quartz and feldspar. Recently, research on new materials such as non-hazardous wastes and natural rocks have been focused on replacing traditional constituents without changing the process or quality of the final products. The aim of this study is to investigate the possibility of the use of volcanic basalt rock in porcelain production. Quartz was progressively replaced by up to 20 wt.% basalt in a traditional porcelain composition. The samples were sintered in an electric furnace with a heating rate of 5 °K minute⁻¹ at 1100, 1150, 1200, 1250 and 1300 °C for 2 h. The effects of this substitution were investigated by measuring the linear shrinkage, bulk density and apparent porosity. The sintered samples were also characterized by X-ray diffraction (XRD) and scanning electron microscopy (SEM) analysis. The effects of this substitution on sintering and microstructural properties are studied. According to the experimental results linear shrinkage and bulk density values were decreased and the apparent porosity ratios were increased by substitution of quartz by basalt. XRD analysis showed that there are three phases consisting of albite, quartz and mullite at the final basalt containing bodies and mullite peaks were increased by increasing the basalt content. SEM studies revealed that there were unresolved quartz, meta-kaolen and mullite in a glassy matrix.

Key words: Sintering, Porcelain, Mullite.

Introduction

Porcelain stoneware tiles are very strongly sintered ceramic materials with water absorption and open porosity close to zero. They possess perfect physical and mechanical properties such as high hardness, abrasion resistance and bending strength [1]. The great development of porcelain stoneware tile was in the 80s as a very compact vitrified product with a high technical performance. Porcelain tiles are made from clay, fluxing agent and filler. Usually the clay is kaolinite, the fluxing agent is feldspar and the filler is quartz [2]. Formulations of triaxial porcelain (SiO₂-Al₂O₃-KNaO) usually involve 25 wt.% of the plastic component, 25 wt.% silica and 50 wt.% feldspar (generally sodium feldspar) for soft porcelain and 50 wt.% of clay, 25 wt.% silica and 25 wt.% feldspar (generally potassium feldspar) for hard porcelain [3]. Firing bodies containing these three components result in a grain and bond microstructure consisting of coarse quartz grains held together by a finer bond or matrix consisting of mullite crystals and a glassy phase [2, 4]. Mullite is the only stable phase in the Al₂O₃-SiO₂ system at atmospheric pressure. The mullite phase is believed to play a significant role in the development of traditional and advanced ceramics [5].

Basalt is a gray to black, fine grained volcanic rock which is the major constituent of oceanic islands and a common component of the continental masses as well [6-8]. Basalt is the most common type of extrusive igneous rock and the most common rock type at the Earth's surface. Most basalt is volcanic in origin and was formed by the rapid cooling and hardening of the lava flows [9]. Chemically, it is composed of major oxides: silica, alumina, iron oxide, calcia, magnesia, and of lesser importance, soda, potassia, titania and manganese and phosphorus oxides, as well as trace amounts of other species. Plagioclase feldspar and monoclinic pyroxene, normally augite, are two major minerals, with magnetite, olivine and certain other accessory minerals often present [6-8].

Although much research has been performed on using alternative materials replacing quartz with such as fly ash, pyrophyllite, zeolite and agate rejects (scrap) for porcelain bodies [5, 10-13], not much effort has been made to use basalt in porcelain. Basalt containing a large amount of SiO₂ and Al₂O₃ can be a good raw material for porcelain. The price of conventional raw materials used in porcelain production is higher than that of basalt. Quartz is harder than basalt, which means its crushing and milling cost is higher. The hardness of basalt is 5-6 according to Mohs scale [14], the quartz's hardness is 7 on the same scale [15]. Therefore, basalt addition provides a lower raw material preparation cost and as proposed in this study lower sintering temperatures, which mean a lower production cost.

*Corresponding author:
Tel : +90 264 295 5768
Fax: +90 264 295 5601
E-mail: symaz@sakarya.edu.tr

In the present study, quartz was progressively replaced by 5, 10, 15 and 20 wt % basalt in traditional porcelain consisting of 50% kaolinitic clay, 25% quartz and 25% feldspar. The effect of such substitutions on the shrinkage, bulk density, porosity and phase evolution in relation to the sintering temperature was studied. Some selected samples were examined for microstructural changes.

Experimental

A basic porcelain composition consisting of 50% kaolin, 25% potassium-feldspar and 25% quartz was selected. Instead of quartz, basalt was used in the selected porcelain composition. Basalt obtained from the Middle Anatolia region of Turkey was used in the studies. Kaolin and potassium-feldspar were supplied from the Celvit ceramic Company, Turkey. Four compositions, marked PB0, PB5, PB10, PB15 and PB20 were studied. The compositions of the raw materials and the marking system are shown in Table 1. Each composition was ball-milled in rubber-lined ceramic jars for 2 h using zirconium oxide balls and distilled water as the milling media and then sieved to pass through 38 μm . After drying, the mixtures were granulated in moist conditions and then semi dry pressed at 23 MPa to prepare specimens of 8 mm in diameter and 10 mm thick. The samples were sintered in an electric furnace with a heating rate of 5 $^{\circ}\text{K}$ minute^{-1} at 1100, 1150, 1200, 1250 and 1300 $^{\circ}\text{C}$ for 2 h. Then, the sintered samples were cooled to room temperature in the furnace.

After sintering, the sintered samples were subjected to physical tests such as sintering shrinkage, apparent porosity and bulk density. Bulk density and percent apparent porosity of the fired samples were measured using the conventional liquid displacement method according to Archimedes's principle. The crystalline phases of the sintered samples were identified by X-ray diffraction analysis (XRD, JEOL MDI/JADE6) with $\text{Cu K}\alpha$ ($\lambda = 1.54056 \text{ \AA}$) radiation. The micro structural characterization of basalt powder and fracture surfaces of sintered samples was examined using a JEOL JSM 5600 scanning electron microscopy (SEM) with an energy dispersive X-ray spectrometer (EDX) attachment.

Table 1. Porcelain compositions in the experimental studies

Sample codes	Raw materials (wt. %)			
	Kaolin	Potassium-feldspar	Quartz	Basalt
PB0	45	30	25	0
PB5	45	30	20	5
PB10	45	30	15	10
PB15	45	30	10	15
PB20	45	30	5	20

Results and Discussion

The macroimages of the sintered specimens were shown in Fig. 1. As shown in Figure 1, the color of the specimens becomes darker with an increase in the basalt content of the porcelain bodies because of the coloring effect of iron in basalt [16]. The results of the chemical analysis of the raw materials are given in Table 2. The chemical analysis results indicate that quartz used in this study is relatively pure. In addition to SiO_2 and Al_2O_3 , basalt contains some other oxides such as MgO , Fe_2O_3 , CaO , etc. Kaolin and potassium-feldspar are of normal type generally used in the porcelain body. An XRD pattern of basalt powder replaced by quartz in porcelain bodies is shown in Fig. 2. The main crystalline phases in the basalt were found to be augite $[(\text{CaFeMg})\text{SiO}_3]$, diopside $[(\text{CaMg}(\text{SiO}_6))]$, anorthite $[(\text{CaAl}_2\text{Si}_2\text{O}_8)]$ and pigeonite $[(\text{MgFeCa})(\text{Si}_2\text{O}_6)]$ as reported in the literature [6-8]. Fig. 3 shows the SEM microstructure of the basalt used.

The oxide compositions of all the batches were calculated on the calcined basis and the results are given

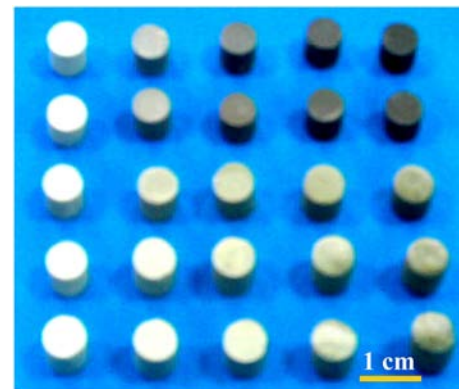


Fig. 1. Macroimages of test specimens a) From left to right an increase in basalt content b) sintering temperature increases from top to bottom.

Table 2. The chemical compositions of the raw materials

	Raw materials (wt. %)			
	Kaolin	Potassium-feldspar	Quartz	Basalt
SiO_2	48	70,93	99,45	45,88
Al_2O_3	37	18,28	0,35	18,2
Fe_2O_3	0,75	0,09	0,1	9,95
TiO_2	-	0,13	-	-
CaO	-	0,5	0,1	9,28
MgO	-	-	-	6,62
Na_2O	-	9,55	-	4,76
K_2O	1,85	0,24	-	1,64
P_2O_5	-	-	-	1,04
L.O.I.*	12,38	0,28	-	2,63

*Loss on ignition

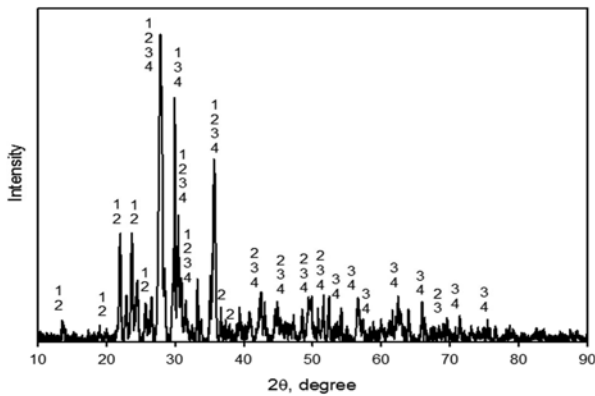


Fig. 2. XRD pattern of basalt (1 = Augite $[(CaFeMg)SiO_3]$, 2 = Pigeonite $[(MgFeCa)(MgFe)(Si_2O_6)]$, 3 = Anortite $[(CaAl_2Si_2O_8)]$, 4 = diopside $[(CaMg)(SiO_6)]$).

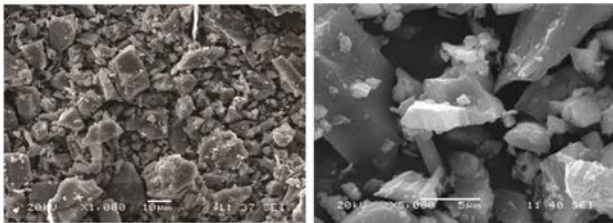


Fig. 3. The SEM microstructure of basalt powders.

in Table 3. From Table 3 it may be noted that, with a progressive addition of basalt by replacing quartz, the alumina content of the batches increases, followed by a decrease in silica content. The percentage of other mineralizing oxides, such as Fe_2O_3 , CaO and MgO are also on the higher side in basalt-containing batches, although there are no significant changes in alkali content.

The variation in percent linear shrinkage with sintering temperature is represented in Fig. 4. From the figure, it can be observed that the standard porcelain composition (PB0) did not show any significant change in the linear shrinkage up to 1200 °C. Above this temperature, linear shrinkage decreases with sintering temperature. A similar trend was observed for the basalt-containing compositions (PB5, PB10, PB15 and PB20) too. The linear shrinkage of PB10, PB15 and PB20 porcelain compositions suddenly decreased at 1200 °C, beyond which the curve is almost flat. The PB20 specimens which present the highest basalt content with respect to other bodies, showed the lowest shrinkage values above 1200 °C. Substitution of quartz by basalt in a normal porcelain body decreases the linear shrinkage, in the entire temperature range of heating (1200-1300 °C). This may be attributed to the presence of fluxing alkaline earth and other oxides in basalt, which enter the liquid phase. When the liquid phase evaporates with a basalt addition and sintering temperature, the linear shrinkage decreases and volume expansion occurs. It is possible that, there is an over firing as reported [17].

The variation in bulk density with heating temperature

Table 3. Oxide compositions of the experimental bodies

Oxide constituents (wt. %)	Batches				
	PB0	PB5	PB10	PB15	PB20
SiO_2	71,8	69,06	66,31	63,55	60,78
Al_2O_3	23,55	24,53	25,52	26,5	27,49
TiO_2	0,05	0,05	0,05	0,05	0,05
Fe_2O_3	0,41	0,94	1,46	1,99	2,51
CaO	0,19	0,67	1,16	1,65	2,14
MgO	-	0,35	0,7	1,06	1,41
Na_2O	3,04	3,29	3,55	3,81	4,07
K_2O	0,96	1,05	1,14	1,22	1,31
P_2O_5	-	0,06	0,11	0,17	0,22

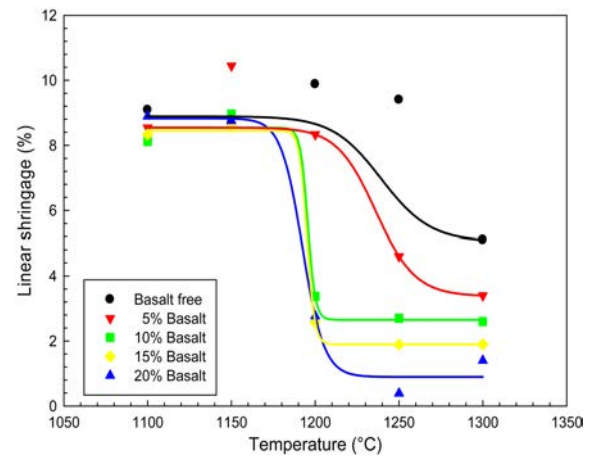


Fig. 4. Linear shrinkage of the sintered samples from 1100 to 1300 °C.

is given in Fig. 5. PB0, PB5 and PB10 porcelain compositions showed an increasing trend in their bulk density with temperature due to increased consolidation with temperature. This phenomenon was also observed by Dana et al. [10]. Basalt melts between 984 -1260 °C according to its chemical composition [6]. In our studies, the melting point for a 100% basalt ceramic body produced in the same conditions with the porcelain compositions was observed at 1200 °C. The reason that the bulk density of the bodies PB15 and PB20 increases with basalt addition up to 1200 °C is that the liquid phase as of fluxing alkaline earth and other oxides in basalt evaporates above this temperature and bulk densities decreases for these compositions. Increasing the basalt addition and sintering temperature revealed more gas output and evaporation.

Fig. 6 shows the effect of sintering temperature on the apparent porosity that reduces with increasing sintering firing temperature in all porcelain compositions. When the apparent porosity values are between 0.71-8.69% wt. for all compositions, the lowest porosity was detected in the basalt-free porcelain composition (PB0). As the basalt content in the body increases, like apparent porosity also increased according to the basalt-free

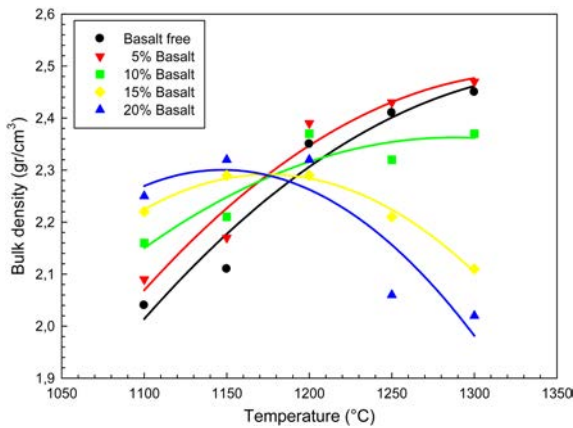


Fig. 5. Bulk density of the sintered samples from 1100 to 1300 °C.

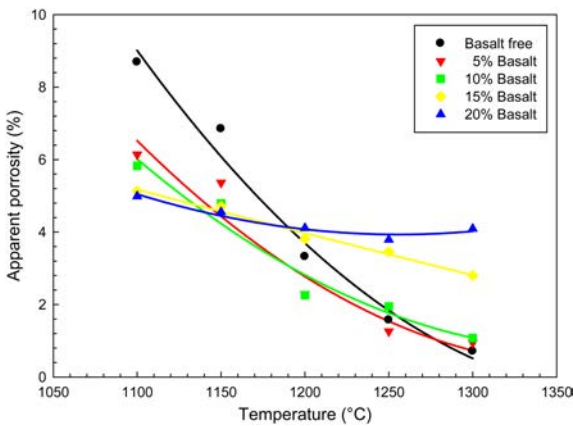


Fig. 6. Apparent porosity of the sintered samples from 1100 to 1300 °C.

composition. This may be due to evaporation of the liquid phase, which results in more gas output and evaporation by adding basalt and increasing the sintering temperature.

In order to investigate the crystalline phases, XRD patterns of samples PB0 and PB15 sintered at all temperature for 2 h are shown in Fig. 7. XRD pattern for compositions PB0 and PB15 indicate that mullite ($3\text{Al}_2\text{O}_3 \cdot 2\text{SiO}_2$), quartz (SiO_2) and albite ($\text{NaAlSi}_3\text{O}_8$) were the crystalline phases. At lower sintering temperatures, mullite, quartz and albite were detected in the PB0 porcelain. As the intensity of the mullite peak rises with the sintering temperature the albite phase could not be seen at above 1200 °C. It is possible that albite and alumina in the glassy phase induce mullitization due to an increase in fluidity and diffusion as reported in the literature [3].

The phases such as mullite, quartz, albite can be seen in the basalt containing porcelain bodies as in the standard porcelain. However, the amount of albite in the body sintered at low temperatures is greater than the standard composition and increases with increasing amounts of basalt. An increase in the amount of basalt in the composition resulted in a reduction in the silica content of porcelain bodies, so the peak intensity of quartz was decreased.

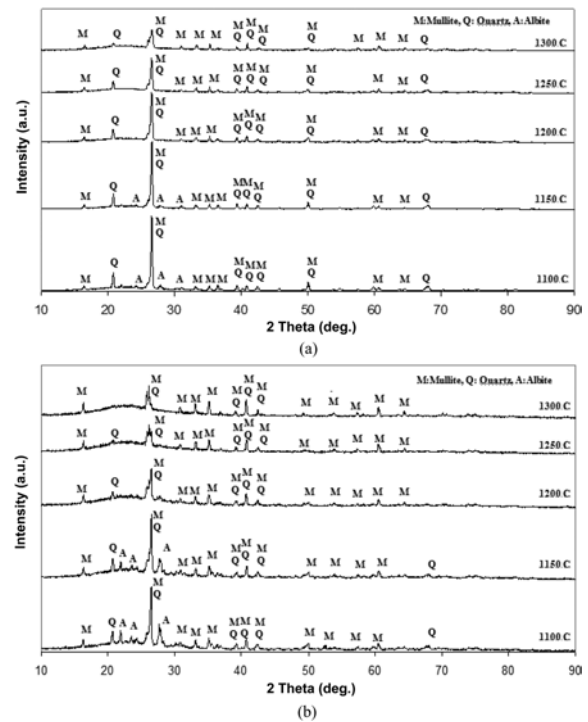


Fig. 7. XRD patterns of the porcelain compositions: (a) PB0, (b) PB15.

When the basalt content in the porcelain body and the fluxing alkaline earth of compositions increase, more peaks and peaks intensities of albite are observed. Above 1200 °C quartz and mullite phases are only observed.

In the literature ions such as Ti^{+4} and Fe^{+3} increased the mullitization have been reported and this case shows the effect of ions is caused by the nucleation centers [3, 18]. In our study, with increasing amounts of basalt in the porcelain bodies an increase in mullite peak intensity was detected. These results are ascribed to the increasing iron content as expressed above.

Scanning electron micrographs of polished and etched specimens sintered at 1300 °C are shown in Fig. 8. The dominant phase is mullite in Al_2O_3 and SiO_2 containing ceramic compositions [19]. The microstructures of all the porcelain bodies in general consists of unresolved quartz and mullite in a glassy matrix. Two types of mullite (primary and secondary) are generally seen in the porcelain microstructures. The most seen type 'primary mullite', which is formed directly from clay is observed in these micrographs (Fig 8). The primary mullite transforms to igneous type 'secondary mullite' at 1300 °C [10, 20]. A small amount of secondary mullite was found in Fig. 8(b) and (d). It was found that 1300 °C is not sufficient for the formation of secondary mullite as reported in the literature [10, 19-21].

EDX analyses were performed with microstructural observations, which supported the identification of the phases. The results of these analyses are shown in Fig. 9 and Table 4.

In the SEM microstructure of etched surfaces of

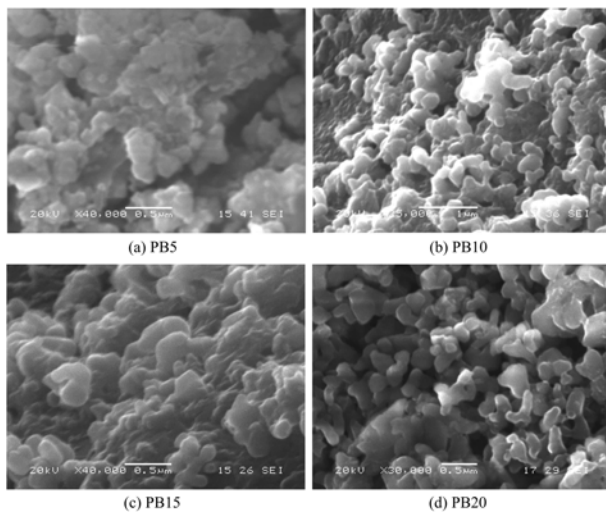


Fig. 8. SEM micrographs of polished and etched specimens of different compositions fired at 1300 °C (a-d). Polished surfaces etched using 5% HF in ethanol for 120 s.

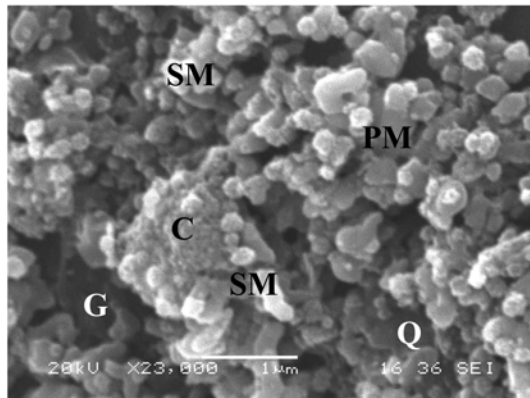


Fig. 9. SEM micrograph of a polished and etched specimen fired at 1300 °C (PB5).

porcelain samples after polishing, some regions were detected which have agglomerated grains (Figs. 8 and 9). These regions are thought to be metakaolen. Metakaolen consists of an $\text{Al}_2\text{O}_3 \cdot 2\text{SiO}_2$ stoichiometric formula. As seen from the chemical formula of metakaolen, Al and Si ratio are close to each other. In the area of SEM microstructures of the regions containing agglomerated grains in which like Al and Si ratios are close to one another in the EDS analysis is considered to be remaining metakaolen which has not transformed to mullite. This case study has been also identified by Demirkiran [22].

Conclusions

From the present investigations, the following conclusions are drawn:

1. It was found that the main crystalline phases in the basalt replacing quartz in the porcelain bodies were augite $[(\text{CaFeMg})\text{SiO}_3]$, diopside $[(\text{CaMg}(\text{SiO}_6))]$, anortite $[(\text{CaAl}_2\text{Si}_2\text{O}_8)]$ and pigeonite $[(\text{MgFeCa})(\text{MgFe})(\text{Si}_2\text{O}_6)]$.

Table 4. EDX analysis of selected regions of PB5 in the SEM micrograph (Fig. 9)

Letters	Main Phase	Secondary Phase	Elements
PM	Primary Mullite	Clay relicts	Si, Al, O
SM	Secondary Mullite	Glass phase, feldspar relict	Si, Al, O, K, Na
G	Glass	Clay relict, mullite	Si, Al, O, K, Na
Q	Quartz	-	Si, O
C	Clay relict (metakaolin)	-	Si, Al, O

2. With substitution of quartz by basalt in a normal porcelain body, no significant change in the linear shrinkage up to 1200 °C was detected. Above this temperature, the linear shrinkage decreases with sintering temperature. This may be due to the formation of a liquid phase due to the presence of fluxing alkaline earth and other oxides in the basalt which evaporate.

3. The bulk density shows an increasing trend with temperature due to increased consolidation for PB0, PB5 and PB10 porcelain compositions at all sintering temperatures. The bulk densities of PB15 and PB20 decrease above 1200 °C because of the evaporation of a liquid phase. Gas output and evaporation is increased with the addition of basalt.

4. It was observed that, the higher the sintering temperature, the lower apparent porosity became in all porcelain compositions.

5. The crystalline phases of all porcelain bodies were detected as mullite, quartz and albite phases up to a sintering temperature of 1200 °C. At higher temperatures, only quartz and mullite phases are observed. The mullite content increases with the addition of basalt in place of quartz due to nucleation center effect of Fe^{+3} ions on mullitization.

6. The microstructure of porcelain bodies consists of unresolved quartz, primary mullite with a lesser amount of secondary mullite in a glassy matrix. Agglomerated grains containing regions thought to be metakaolen were also detected in the SEM microstructure.

Acknowledgements

The authors would like to express their gratitude to Sakarya University Engineering Faculty and Prof. Dr. Cuma Bindal for supporting this work. The authors express their grateful thanks to Müberra Yılmaz (MSc) for assisting with writing, checking and experimental assistance.

References

1. K. Galos, Appl. Clay. Sci. 51 (2011) 74-85.
2. J.M. Pe' rez, J. Ma. Rinco'n and M. Romero, Ceram. Int. 38 (2012) 317-325.

3. E. Kamseu , C. Leonelli , D.N. Boccaccini , P. Veronesi , P. Miselli, G. Pellacani and U. C. Melo, *Ceram.Int.* 33 (2007) 851-857.
4. L. Carbajal, F. Rubio-Marcos, M.A. Bengochea and J.F. Fernandez, *J. Euro. Ceram. Soc.* 27 (2007) 4065-4069.
5. T.K. Mukhopadhyay, S. Ghosh, S. Ghatak and H.S. Maiti, *Ceram.Int.* 32 (2006) 871-876.
6. G.H. Beall and H. L. Rittler, *Am. Ceram. Soc. Bull.* 55 (1976) 579-582.
7. S. Yilmaz, O.T. Ozkan and V. Gunay, *Ceram.Int.* 22 (1996) 477-481.
8. G. Bayrak and S. Yilmaz, *Ceram.Int.* 32 (2006) 441-446.
9. A. Ibrahim, S. Faisal and N. Jamil, *Cons. Build. Mat.* 23 (2009) 498-506.
10. K. Dana, S. Das and S.K. Das, *J. Euro. Ceram. Soc.* 24 (2004) 3169-3175.
11. S. Yuruyen and H.O. Toplan, *Ceram.Int.* 35 (2009) 2427-2433.
12. A.S. Demirkiran, R. Artir and E. Avci, *J. Mat. Proces. Tech.* 203 (2008) 465-470.
13. T.K. Mukhopadhyay, S. Ghatak and H.S. Maiti, *Ceram.Int.* 35 (2009) 2555-2562.
14. S.L. Correia, G. Dienstmann, M.V. Folgueras and A.M. Segadaes, *J. Hazard. Mat.* 163 (2009) 315-322.
15. I. Tore and N. Ay, *Key.Eng.Mat.* 264-268 (2004) 1701-1704.
16. J. Molera, T. Pradell, M. Vendrell-Saz, *Appl. Clay Sci.* 13 (1998) 187-202.
17. C. Hosten and H. Cimilli, *Int. J. Miner. Process.* 91 (2009) 81-87.
18. N. Montoya, F.J. Serrano, M.M. Reventós, J.M. Amigo, J. Alarcón, *J. Euro. Ceram. Soc.* 30 (2010) 839-846.
19. A.P. Luz and S. Riberio, *Ceram.Int.* 33 (2007) 761-765.
20. W.E. Lee and Y. Iqbal, *J. Euro. Ceram. Soc.* 21 (2001) 2583-2586.
21. S.R. Bragança and C.P. Bergmann, *J. Euro. Soc.* 24 (2004) 2383-2388.
22. A.S Demirkiran, Ph.D. Thesis, Sakarya University, Sakarya -Turkey, 2006.